Global Biogeochemical Cycles

RESEARCH ARTICLE
10.1029/2024GB008174

Key Points:

- Changes in bacterial community diversity, taxa abundance and interspecific interaction contributed the most to soil P fraction variation
- Bacterial C demand facilitated soil P turnover by mediating their organic P mineralization potential
- Bacterial functioning on P cycling predominated during early succession stages but attenuated when higher plant-fungal symbionts emerged

Supporting Information:

Supporting Information may be found in the online version of this article.

Correspondence to:

H. Bing and L. Fang,
hjbing@imde.ac.cn;
flinc629@hotmail.com

Citation:

Wang, Y., Bing, H., Moorhead, D. L., Hou, E., Wu, Y., Wang, J., et al. (2024). Bacterial community structure modulates soil phosphorus turnover at early stages of primary succession. *Global Biogeochemical Cycles*, *38*, e2024GB008174. https://doi.org/10.1029/2024GB008174

Received 17 MAR 2024
Accepted 17 SEP 2024

Author Contributions:

Conceptualization: Daryl L. Moorhead, Jipeng Wang, Tianyi Qiu, Zhongmin Dai, Hans Lambers, Peter B. Reich, Linchuan Fang
Formal analysis: Yuhan Wang, Chengjiao Duan
Funding acquisition: Haijian Bing, Yanhong Wu, Peter B. Reich, Linchuan Fang
Investigation: Yuhan Wang, Haijian Bing, He Zhu
Validation: Chengjiao Duan
Visualization: Yuhan Wang, Qingliang Cui, Zhiqin Zhang
Writing – original draft: Yuhan Wang, Haijian Bing, Linchuan Fang
Writing – review & editing: Haijian Bing, Daryl L. Moorhead, Enqing Hou, Yanhong Wu, Jipeng Wang, Tianyi Qiu, Zhongmin Dai, Wenfeng Tan,

© 2024. American Geophysical Union. All Rights Reserved.

Bacterial Community Structure Modulates Soil Phosphorus Turnover at Early Stages of Primary Succession

Yuhan Wang[1], Haijian Bing[2], Daryl L. Moorhead[3], Enqing Hou[4], Yanhong Wu[2], Jipeng Wang[5], Chengjiao Duan[6], Qingliang Cui[6], Zhiqin Zhang[7], He Zhu[2], Tianyi Qiu[1,7], Zhongmin Dai[8], Wenfeng Tan[9], Min Huang[1], Hans Lambers[10], Peter B. Reich[11,12], and Linchuan Fang[1,6]

[1]Key Laboratory of Green Utilization of Critical Non-metallic Mineral Resources, Ministry of Education, Wuhan University of Technology, Wuhan, China, [2]Institute of Mountain Hazards and Environment, Chinese Academy of Sciences, Chengdu, China, [3]Department of Environmental Sciences, University of Toledo, Toledo, OH, USA, [4]Key Laboratory of Vegetation Restoration and Management of Degraded Ecosystems, South China Botanical Garden, Chinese Academy of Sciences, Guangzhou, China, [5]CAS Key Laboratory of Mountain Ecological Restoration and Bioresource Utilization and Ecological Restoration and Biodiversity Conservation Key Laboratory of Sichuan Province, Chengdu Institute of Biology, Chinese Academy of Sciences, Chengdu, China, [6]State Key Laboratory of Soil Erosion and Dryland Farming on the Loess Plateau, Institute of Soil and Water Conservation CAS and MWR, Yangling, China, [7]College of Natural Resources and Environment, Northwest A&F University, Yangling, China, [8]Institute of Soil and Water Resources and Environmental Science, College of Environmental and Resource Sciences, Zhejiang University, Hangzhou, China, [9]State Environmental Protection Key Laboratory of Soil Health and Green Remediation, College of Resources and Environment, Huazhong Agricultural University, Wuhan, China, [10]School of Biological Sciences, University of Western Australia, Perth, WA, Australia, [11]Institute for Global Change Biology and School for Environment and Sustainability, University of Michigan, Ann Arbor, MI, USA, [12]Department of Forest Resources, University of Minnesota, St. Paul, MN, USA

Abstract Microbes are the drivers of soil phosphorus (P) cycling in terrestrial ecosystems; however, the role of soil microbes in mediating P cycling in P-rich soils during primary succession remains uncertain. This study examined the impacts of bacterial community structure (diversity and composition) and its functional potential (absolute abundances of P-cycling functional genes) on soil P cycling along a 130-year glacial chronosequence on the eastern Tibetan Plateau. Bacterial community structure was a better predictor of soil P fractions than P-cycling genes along the chronosequence. After glacier retreat, the solubilization of inorganic P and the mineralization of organic P were significantly enhanced by increased bacterial diversity, changed interspecific interactions, and abundant species involved in soil P mineralization, thereby increasing P availability. Although 84% of P-cycling genes were associated with organic P mineralization, these genes were more closely associated with soil organic carbon than with organic P. Bacterial carbon demand probably determined soil P turnover, indicating the dominant role of organic matter decomposition processes in P-rich alpine soils. Moreover, the significant decrease in the complexity of the bacterial co-occurrence network and the taxa-gene-P network at the later stage indicates a declining dominance of the bacterial community in driving soil P cycling with succession. Our results reveal that bacteria with a complex community structure have a prominent potential for biogeochemical P cycling in P-rich soils during the early stages of primary succession.

Plain Language Summary Microbial P turnover regulates soil P biogeochemical cycling during primary succession. Here, we revealed that the changes in bacterial community diversity, taxa abundance, and interspecific interaction were better predictors of soil P fraction variation than P-cycling gene abundances along a 130-year glacial chronosequence. The close link of organic P mineralization genes to SOC shows that bacterial carbon demand actuated soil P turnover through organic matter mineralization. Furthermore, we found that bacterial functioning on soil P cycling predominated during early succession stages, which attenuated with the dominance of higher plants and plant-fungal symbionts.

1. Introduction

Under climate warming, increasing bare land surfaces are exposed in alpine regions, which provides a platform for ecosystem establishment and succession (Bosson et al., 2023; Ficetola et al., 2024). Phosphorus (P) is an essential nutrient for metabolism, and P deficiency can limit ecosystem productivity and impair terrestrial carbon sequestration (Elser et al., 2007; Luo et al., 2022). Unlike carbon (C) and nitrogen (N) that are readily accessible through biological processes, P enters natural ecosystems primarily originating from the slow weathering of

Min Huang, Hans Lambers, Peter B. Reich, Linchuan Fang

bedrock, rendering P an ultimate limiting nutrient for primary productivity and ecological succession (Darcy et al., 2018; Laliberté et al., 2012). During the early stages of succession, microbial communities are crucial in driving P biogeochemical cycling due to their higher capacity to facilitate organic matter mineralization and inorganic P solubilization compared to more established ecosystems (Bergkemper et al., 2016; Richardson & Simpson, 2011). At newly exposed glacier forefields, these microbial communities can sustain their metabolic activities by utilizing low concentrations of organic matter present beneath the glacier (Bardgett et al., 2007; Hood et al., 2015), thereby dictating soil P turnover (van der Heijden et al., 2008). The influences of microbial communities on soil P dynamics are mediated by the shifts in microbial community composition and functional potentials (Liang et al., 2020; Louca et al., 2018). However, how and to what extent the microbial community initiates soil P cycling at early stages of primary succession remains unclear and deserves in-depth research.

Functional genes encoded by microbes regulate diverse P metabolic pathways that drive soil P biogeochemical cycling. The genes encoding enzyme exudation (e.g., phosphatase, phytase and C-P lyase) and organic anion release directly regulate organic P (P_O) mineralization and inorganic P (P_i) solubilization, respectively (Richardson & Simpson, 2011; Siles et al., 2022). The most common gene involved in soil P_O mineralization is the *phoD* gene, encoding alkaline phosphatase, which has a high capacity to mineralize organophosphates (Wang, Bu, et al., 2021). The *phn* operon regulates the C-P lyase, targeting phosphonate compounds in forest soils (Siles et al., 2022). In addition, the genes of *gcd* and *pqqC* encoding glucose dehydrogenase and pyrroloquinoline quinone synthase, respectively, govern inorganic phosphate solubilization in soils (Liang et al., 2020; Wu et al., 2019), and the gene *ppx* encoding exopolyphosphatase and the gene *ppk3* encoding polyphosphate kinase are associated with the hydrolysis and biosynthesis of polyphosphate (polyP), respectively (Albi & Serrano, 2016). The abundance of the P-cycling functional genes has been increasingly used to predict the microbial potential for soil P turnover because the changes in gene abundances are considered to be tightly coupled with the specific P cycling processes in soils (Dai et al., 2020; Escalas et al., 2019). However, bare land soils are characterized by relatively abundant P but limited content of organic matter, which constricts microbial growth and metabolism by the availability of C in the soils at the early stage of primary succession (Heuck et al., 2015). Thus, microbes may mineralize soil organic matter to alleviate C limitation, and as a side product, the bioavailable P fraction may be increased in soils during organic matter decomposition (McConnell et al., 2020; Spohn & Kuzyakov, 2013). This will lead to the decoupling of P-cycling functional genes and their regulated enzymes with soil P fractions, owing to the possibility of the constitutive expression of microbial functional genes and functional redundancy (Wang et al., 2016; Xu et al., 2022).

In addition to C limitation, the composition and diversity of microbial communities are directly regulated by the forms and quantity of C in soils (Liu et al., 2022; Yu et al., 2023), and the C-driven variation in microbial structure is intimately related to soil P transformation (Chen et al., 2020; Heuck et al., 2015). A more active, abundant, and diverse soil microbial community can promote mycorrhizal formation and the exudation of more organic acids and phosphatases to increase soil P availability (Qiu et al., 2024; Wu et al., 2019). Meanwhile, changes in the composition of bacterial community, such as increasing prevalence of copiotrophic bacteria (e.g., Firmicutes and Bacteroidetes), may directly stimulate the potential of P_i utilization (Oliverio et al., 2020). Moreover, the interspecific cooperation between bacterial taxa can influence the composition and size of soil P fractions, and thus mediate the biogeochemical processes of soil P turnover (Gaiero et al., 2021). It is well realized that soil P fractions tend to be dominated more by P_O than P_i during primary succession (Walker & Syers, 1976). However, there remains considerable uncertainty regarding the pathways of microbes, particularly bacteria, acting as pioneer colonizers in driving P turnover in P-rich soils during vegetation succession, including questions of the role of changes in bacterial community structure or functional potential. Advancing knowledge on these topics will provide a new framework to understand the microbial-mediated P cycling processes in P-rich soils, thereby elevating primary succession theory (Ficetola et al., 2021; McConnell et al., 2020).

Here, we selected the Hailuogou Glacier chronosequence on the eastern Tibetan Plateau to unravel the successional patterns of bacterial community structure and P-cycling functional genes and to decipher the ways bacteria mediate soil P cycling during primary succession. A recent study detected a certain concentration of organic C in soils at the initial bare and pioneer vegetation stage (Yu et al., 2023), which provides a substrate for microbial community colonization and succession in the glacier forefield (Bai et al., 2020). The transition from pioneer species to climax plant communities profoundly alters microbial communities and their functions in soils (Ficetola et al., 2021), particularly within the rhizosphere environment, where microbial succession is strongly shaped by plant-soil interactions (Kardol et al., 2006; Zhou et al., 2022). Moreover, despite the rapid weathering

of primary mineral phosphates, soil P_O accumulation markedly increases along with the microbial P fraction and soil P availability during primary succession (Wang et al., 2016; Zhou et al., 2019). We therefore hypothesized that in P-rich soils, the structure of the bacterial community was more closely linked to soil P cycling than their functional potential related to P turnover. Furthermore, we proposed that bacteria primarily exploited the P_i fractions during the early stages of succession, subsequently transitioning to the utilization of P_O compounds at the later stages. As such, bacteria can initiate soil P cycling in the newly exposed soils, but this role decreases with soil P depletion and plant development with succession.

2. Materials and Methods

2.1. Study Area and Sample Collection

The Hailuogou Glacier chronosequence (~3,000 m above sea level, 29°34′00″N, 101°57′00″E) is located on the eastern slope of Gongga Mountain, eastern Tibetan Plateau (Figure S1a in Supporting Information S1). The Hailuogou Glacier has been retreating since the end of the last Little Ice Age (1850 AD), and a ~130-year soil development gradient has formed within a ~2 km length and ~100 m gap in altitude. The climate in the study area is controlled by the Asian monsoon with a mean annual temperature of 4°C and a mean annual precipitation of 1947 mm. There is similar parent material (granitoid) and gentle topography along the chronosequence. We selected six successional stages along the chronosequence and a nearby reference site with mature coniferous forests (Figure S1b in Supporting Information S1). The soils are classified as Regosols at Stages 1–6 and Podzols at the reference site (Wang, Wu, et al., 2021). Stages 1 and 2 (early stage) were exposed in 2010 and 1980, respectively, and are colonized by the symbiotic N_2-fixing species *Astragalus mahoshanicus* and *Hippophae rhamnoides*. Stages 3 and 4 (intermediate stage) were exposed in 1970 and 1958, respectively, were initially colonized by *A. mahoshanicus* and *H. rhamnoides* and are now dominated by the deciduous trees *Populus purdomii* and *Salix spp*. Stages 5 and 6 (later stage) were exposed in 1930 and 1890, respectively, were colonized first by *Astragalu/Hippophae* and second by *Populus/Salix*, and are now dominated by the coniferous trees *Abies fabri* and *Picea brachytyla*. The reference site (mature coniferous forest) was exposed for over 1400 years, is dominated by *A. fabri* and has a well-developed understorey community of *Bashania fangiana* (Table 1; Li & Xiong, 1995; Wang et al., 2016).

At each succession stage, we randomly selected four 10 m × 10 m plots (at least 10 m away from each other). Sampling was done in the middle of the growing season. Considering the distinct soil conditions and C sources in the rhizosphere, rhizosheath and bulk soils were collected beneath the plant species and then mixed into one sample at each plot. The soils loosely adhering to fine roots were shaken slightly and collected as bulk soils, and the soils tightly adhering to the fine roots were gently brushed off and collected as rhizosheath soils (Figure S1c in Supporting Information S1). In total, we collected 28 samples (4 replicates × 7 sites) from the rhizosheath and bulk soils. All samples were collected from the topsoil layer (0–10 cm) and passed through a 2-mm sieve to remove gravel and roots. Approximately 2 g of soil was stored at −80°C for high-throughput sequencing, and approximately 50 g of soil was stored at 4°C for the analysis of microbial biomass and extracellular enzyme activities. Other samples were air-dried for the analysis of soil chemical properties.

2.2. Soil Chemical Analysis

Soil water content was determined by oven-drying the soil at 105°C until constant weight. Soil pH was measured in soil suspension by a glass-electrode (InsMark™ IS126, Shanghai, China) with a soil to water ratio of 1:10. The concentration of soil organic carbon (SOC) was measured with an elemental analyzer (Elementar vario MACRO cube, Langenselbold, Germany) after removing carbonates using 0.5 M HCl. The concentration of total P (TP) was measured with an injection pump analyzer (AA3, SEAL Company, Norderstedt, Germany) following the digestion with a mixture of H_2SO_4 and $HClO_4$ (Cui et al., 2019, 2020). The concentration of inorganic P (P_i) was measured as P extractable by concentrated H_2SO_4 in combusted soils, and the concentration of organic P (P_O) was calculated as the difference in P_i extracted by concentrated H_2SO_4 between the combusted and non-combusted soils.

The activities of extracellular enzymes (EEAs) involved in the acquisition of C (β-1,4-glucosidase (BG) and β-D-cellobiosidase (CBH)) and P (phosphatase (AP)) were determined by the microplate fluorometric assay (Cui et al., 2019). Briefly, fresh soils were used to prepare soil suspensions, and 1 mL filtrate was incubated in the dark for 4 hr at 25°C with the respective substrate, control, and standard materials. Fluorescence was measured using a

Table 1
Characteristics of Key Soil Properties Across the Successional Stages With the Corresponding Dominant Plant Species at the Hailuogou Glacier Forefield

Succession stage	Exposure time (years)	Dominant plant species	Location	SWC (%)	pH	SOC (g kg^{-1})	$Soil_{C:P}$ (molar)	$MB_{C:P}$:$Soil_{C:P}$ (molar)
S1	10	*Astragalus mahoshanicus*	Rhizosheath soil	12.5 ± 0.65 c	**7.72 ± 0.05 a**	8.30 ± 0.96 c	23.6 ± 3.0 e	**4.80 ± 1.8 a**
S2	40	*Hippophae rhamnoides*		78.2 ± 0.70 ab	4.93 ± 0.13 c	**310 ± 10 a**	826 ± 37 b	0.095 ± 0.015 a
S3	50	*Populus purdomii*; *Salix spp.*		77.5 ± 0.55 ab	5.84 ± 0.13 b	**323 ± 2.0 a**	**821 ± 5.3 bc**	0.072 ± 0.006 a
S4	62	*Populus purdomii*; *Salix spp.*		**75.3 ± 0.80 ab**	5.67 ± 0.01 b	**237 ± 22 b**	**573 ± 52 c**	0.097 ± 0.026 a
S5	90	*Abies fabri*		79.4 ± 0.75 a	4.27 ± 0.17 d	358 ± 12 a	1356 ± 101 a	0.064 ± 0.025 a
S6	130	*Abies fabri; Picea brachytyla*		80.1 ± 1.05 a	4.57 ± 0.07 cd	340 ± 14 a	1316 ± 76 a	0.051 ± 0.031 a
Ref. Site	>1400	*Abies fabri; Bashania fangiana*		73.8 ± 0.45 ab	4.37 ± 0.02 d	221 ± 18 b	530 ± 14 b	0.24 ± 0.045 a
S1	10	*Astragalus mahoshanicus*	Bulk soil	11.6 ± 0.65 d	**8.60 ± 0.28 a**	8.45 ± 0.49 e	24.5 ± 1.4 d	**24.0 ± 11 a**
S2	40	*Hippophae rhamnoides*		76.1 ± 1.55 ab	4.70 ± 0.14 c	**270 ± 25 b**	863 ± 74 b	0.086 ± 0.014 b
S3	50	*Populus purdomii*; *Salix spp.*		75.5 ± 0.30 a	5.62 ± 0.12 b	**225 ± 8 bc**	**708 ± 21 b**	0.062 ± 0.012 b
S4	62	*Populus purdomii*; *Salix spp.*		**54.1 ± 3.00 c**	5.67 ± 0.08 b	**72.0 ± 11 d**	**190 ± 34 c**	0.51 ± 0.16 b
S5	90	*Abies fabri*		80.2 ± 0.25 a	4.30 ± 0.09 c	359 ± 13 a	1392 ± 100 a	0.063 ± 0.019 b
S6	130	*Abies fabri; Picea brachytyla*		78.6 ± 0.55 a	4.57 ± 0.08 c	336 ± 10 a	1297 ± 73 a	0.069 ± 0.017 b
Ref. Site	>1400	*Abies fabri; Bashania fangiana*		72.4 ± 2.25 b	4.40 ± 0.01 c	179 ± 11 c	519 ± 62 c	0.25 ± 0.11 b

Note. The effects of succession stage and location (rhizosheath and bulk) on the variables were examined by the linear mixed-effects model. Data are presented as mean ± standard error ($n = 4$). Different lowercase letters in each column indicate a significant difference in the variable between the stages ($P < 0.05$). The bold data indicate significant differences between the rhizosheath and bulk soil at each stage ($P < 0.05$). SWC: soil water content, SOC: soil organic carbon, MBC: microbial biomass carbon, MBP: microbial biomass phosphorus, $Soil_{C:P}$: the ratio of SOC to TP, $MB_{C:P}$:$Soil_{C:P}$: the ratio of MBC:MBP to SOC:TP.

multi-function microplate reader (Scientific Fluoroskan Ascent FL, Thermo, Massachusetts, American) with excitation at 365 nm and emission at 450 nm. The EEAs were expressed as nanomoles of substrate released per hour per gram of dry soil (nmol g^{-1} h^{-1}). The concentrations of microbial biomass C and P (MBC and MBP) were analyzed by the chloroform fumigation–extraction method (Brookes et al., 1982; Vance et al., 1987). Conversion coefficients of 0.45 and 0.40 were used to calculate MBC and MBP, respectively (Joergensen, 1996). Specifically, samples for MBC analysis were extracted with 0.5 M K_2SO_4 and quantified using a total organic carbon and total nitrogen analyzer (multi N/C 3100, Analytik Jena GmbH, Thuringia, Germany). Samples for MBP analysis were extracted with 0.5 M $NaHCO_3$ and quantified using a molybdenum blue method with an ultraviolet spectrophotometer (UV3200, Shimadu Corporation, Kyoto, Japan). Available soil P (ASP) was defined as the P determined in the supernatants of the non-fumigated samples. The $MB_{C:P}$/$Soil_{C:P}$ ratio was used to represent substrate quality for microbial metabolism, with higher ratios representing greater microbial C limitation relative to P (Wang, Wu, et al., 2021).

2.3. DNA Extraction and High-Throughput Illumina Sequencing

DNA was extracted from 0.5 g of fresh soil using the ALFA-SEQ Advanced Soil DNA Kit (Guangdong Magigene Biotechnology Co., Guangzhou, China). The concentration and purity of DNA were determined using a Spectrophotometer (NanoDrop One, Thermo Fisher Scientific, Massachusetts, USA) and a Qubit fluorometer (2.0, Thermo Fisher Scientific, Waltham, USA), respectively.

Genomic DNA was used as a template to assess the bacterial community. Targeting primers for the V4-V5 region including 515F (GTGCCAGCMGCCGCGGTAA) and 907R (CCGTCAATTCMTTTRAGTTT) were selected for the determination of 16S rRNA genes, and PCR amplification was performed using TaKaRa Premix Taq® version 2.0 (TaKaRa Biotechnology Co., Dalian, China). Detailed experimental methods are presented in the Supporting Information S1. Principal Coordinate Analysis (PCoA) based on Bray-Curtis distances was used to visualize the bacterial community structure in multidimensional space. The bacterial sequences have been submitted to the National Center for Biotechnology Information with accession number PRJNA814341. The

sequencing quality indicated by rarefaction curves was good to reflect the microbial populations in the study area (Figure S2 in Supporting Information S1).

A total of eight bacterial P-cycling functional genes were identified, including four P_O-mineralization genes (*phnK*, *phoD*, *phoX*, *bpp*), two P_i-solubilization genes (*pqqC*, *cphy*), and two genes related to polyP hydrolysis (*ppx*) and biosynthesis (*ppk3*). Specific information on the primers is shown in Table S1 in Supporting Information S1. Specifically, qualified DNA samples were added to one plate as the sample sourceplate, and the primer and qPCR reagent were added to another plate as the assay sourceplate. Then, the sample source plate and assay source plate reagents were separately added to the micropores of a SmartChip MyDesign Chip (Takara Biomedical Technology, Beijing, China), a high-throughput qPCR chip, using the SmartChip Multisample Nanodispenser (Takara Biomedical Technology, Beijing, China). The qPCR reaction was performed using the SmartChip Real-Time PCR System (WaferGen Biosystems, Fremont, USA). The CT (cycle threshold) values of each gene in each sample were obtained for quality control by the SmartChip Real-Time PCR System (WaferGen Biosystems, Fremont, USA) and Canco software. If the amplification efficiency was <1.8 or >2.2 and the CT values were >31, the analysis was discarded. The absolute quantification of the 16S rRNA genes was obtained by fluorescence quantitative PCR (Roche, LightCycler480II, Basel, Switzerland), and the absolute abundance of different genes was converted from 16S rRNA (Zheng et al., 2018). The CT values of *cphy* in all the samples did not reach the detection limit, and thus its abundance was considered zero.

2.4. Co-Occurrence Network Analysis

Bacterial co-occurrence networks were constructed for both the rhizosheath and bulk soils at the early (N_2-fixing species, Stages 1–2), intermediate (broadleaf species, Stages 3–4) and later (coniferous species, Stages 5–6) successional stages using eight biological replicates. Here, the operational taxonomic units (OTUs) were used to represent bacterial species, and the OTUs appearing less than five times in the eight replicates were discarded. Next, the Spearman correlation matrix of all OTUs was determined using the "HMISC" package in R. The p-value was corrected according to the Benjamini-Hochberg method (Benjamini & Hochberg, 1995), and the threshold was set at 0.01. The threshold of the correlation coefficient was set according to the random matrix theory (Deng et al., 2012). Finally, the networks were visualized in the interactive platform of Gephi (https://gephi.org/). The same procedure was used to construct the taxa-gene-P and taxa-gene networks with the p-value threshold of 0.05. Natural connectivity was introduced as a measure of the robustness of bacterial co-occurrence networks using the "igraph" package in R.

2.5. Statistical Analyses

All analyses were performed using R software (version 3.5.1). A linear mixed-effect model was used to test for differences in soil P status, physicochemical and biochemical properties, and P-cycling gene abundances with plots set as a random factor and succession stage and location as the fixed effects using the "lm4" package, and then the means of variables that were statistically significant in the model were compared by the "emmeans" package ($P < 0.05$). Non-metric multidimensional scaling analysis (NMDS) based on the Bray-Curtis dissimilarity (distance) was used to assess the differences in P-cycling genes across different succession stages using the "vegan" package. The Mantel test was performed to evaluate the impact of bacterial community structure (community composition) and functional potential (gene abundance) on soil P status and other properties by the "linkET" package. Random forest was used to determine the importance of factors influencing available soil P by the "rfPermute" and "randomForest" packages.

3. Results

3.1. Soil Physicochemical and Biochemical Properties

During primary succession, soil conditions undergo dramatic changes characterized by increased soil nutrient levels and significant alterations in P distribution (Table 1, Figure 1). SWC and pH varied significantly along the chronosequence and showed a significant trend of increasing and decreasing with succession, respectively. The SOC concentrations were lowest at Stage 1 and much higher at all other stages. The $Soil_{C:P}$ ratio showed a markedly increasing trend with succession. When aboveground plants were dominated by N_2-fixing (Stages 1–2, early stage) and deciduous species (Stages 3–4, intermediate stage), there were significantly higher concentrations of TP and P_i than at Stages 5–6 (later stage) (Figures 1a and 1c). For P_O and ASP, the concentrations

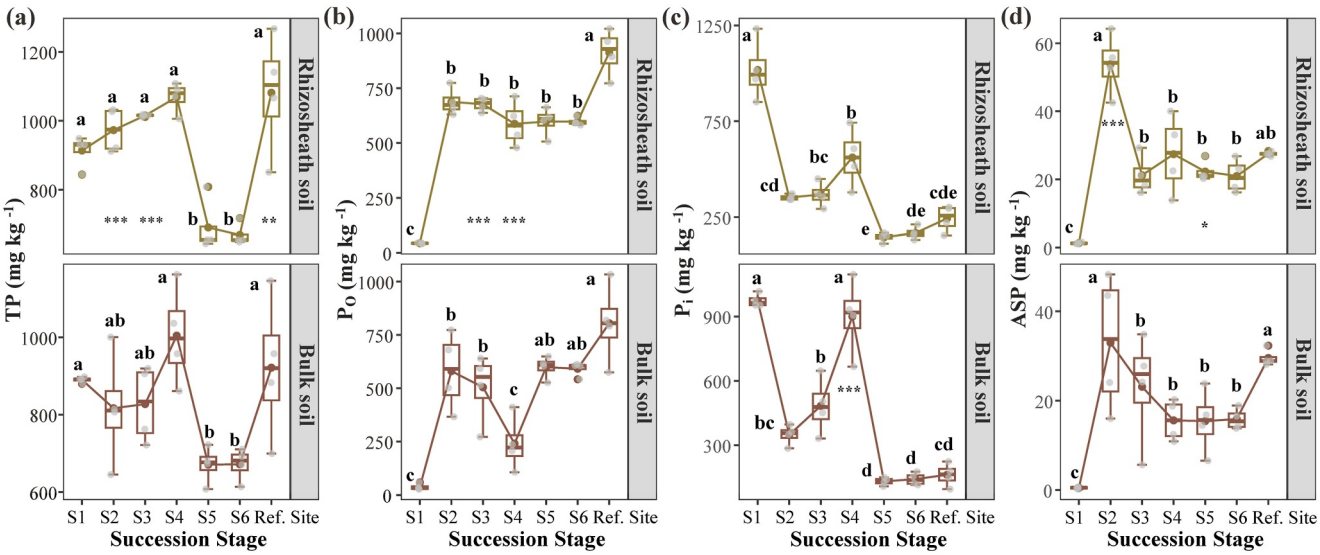

Figure 1. The concentrations of TP, P_O, P_i and ASP in soils (a–d) along the chronosequence and at the reference site. Each box represents the lower and upper quartiles with the medians and means shown as the central lines and solid circles, respectively. Different lowercase letters within a column indicate significant differences along the chronosequence in the bulk or rhizosheath soils ($P < 0.05$). Asterisk indicates significant differences between the bulk and rhizosheath soils at a stage. TP: total phosphorus, P_O: organic phosphorus, P_i: inorganic phosphorus, ASP: available soil phosphorus.

increased after Stage 1 and then stabilized at a relatively lower level at Stages 5–6, and then slightly increased at the reference site (Figures 1b and 1d).

Similarly, soil microbial activities including biomass and exoenzyme activities showed clear succession patterns (Table 1, Figure S3 in Supporting Information S1). The concentrations of MBC and MBP increased markedly from Stage 1 to Stage 2 and then decreased significantly with succession, especially in the bulk soils (Figures S3a and S3b in Supporting Information S1). The ratios of $MB_{C:P}$ and $MB_{C:P}$:$Soil_{C:P}$ did not differ along the chronosequence except for the one higher value in the bulk soils at Stage 1 (Figure S3c in Supporting Information S1). The BG + CBH (C-acquiring enzymes) activities in the rhizosheath soils increased significantly from Stage 1 to Stage 2, while a significant decrease was observed in the bulk soils at Stage 4 and in the rhizosheath soils at the reference site. The AP (P-acquiring enzyme) activities tended to increase with increasing succession stage but were lower at the reference site (Figures S3d and S3e in Supporting Information S1). The $EEA_{C:P}$ ratio was observed to be relatively higher at Stages 2–4 (Figure S3f in Supporting Information S1). The efficiency of C- and P-acquiring enzymes tended to increase with succession stage, peaking in the bulk soils at Stages 3–4 and in the rhizosheath soils at Stages 5–6 at marginal significance, while being lower at the reference site (Figures S3g and S3h in Supporting Information S1).

3.2. Microbial Community Composition and Co-Occurrence Networks

Microbial community structure, such as diversity, composition, and interspecific interaction, was distinct across succession stages (Figure 2). In both the rhizosheath and bulk soils, bacterial diversity indicated by the Chao1 and Shannon index increased from Stage 1 to Stage 4 and then was uniformly lower in older post-glacial sites dominated by conifers (Figure 2a). The bacterial community composition differed massively and clearly among successional stages according to the PCoA (Figure 2b). Specifically, the bacterial communities exhibited marked dissimilarity at Stage 1 (herb-dominated) compared to all other stages, a similarity at Stages 2–4 (shrubs or deciduous species dominance), and once more, distinctiveness at Stages 5–7 (coniferous species dominance). Along the chronosequence, the relative abundance in both the rhizosheath and bulk soils decreased for Proteobacteria (30%–48%), Actinobacteria (2.6%–11%), Bacteroidetes (4.2%–12%), Chloroflexi (0.37%–6.9%) and Gemmatimonadetes (0.29%–1.3%), increased for Acidobacteria (9.2%–46%), Verrucomicrobia (0.69%–3.4%) and Omnitrophicaeota (0.04%–1.2%), and showed a parabolic pattern for Planctomycetes (5.1%–11%), Patescibacteria (0.47%–2.1%) and Nitrospirae (0.02%–1.4%) (Figure 2c). More strikingly, the most abundant bacterial phyla shifted from Proteobacteria to Acidobacteria with increasing succession stage.

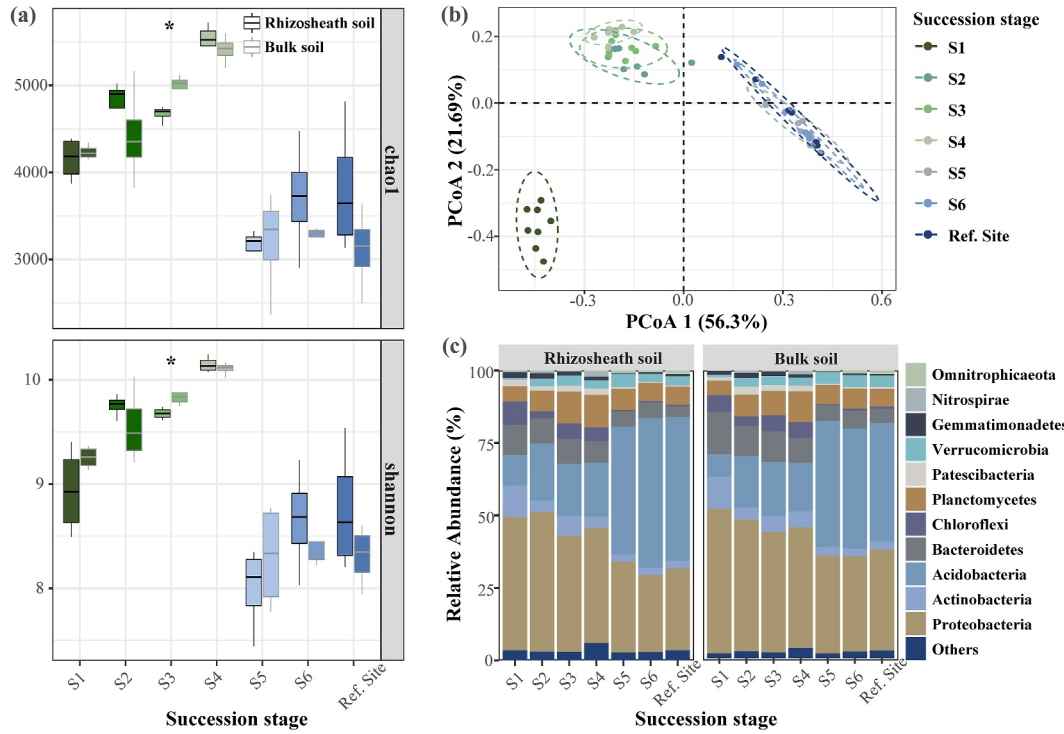

Figure 2. Variations in bacterial community structure along the chronosequence and at the reference site. (a) Chao1 richness and Shannon index. (b) Principal coordinates analysis (PCoA) based on the Bray-Curtis distance. (c) The composition of the bacterial community at the phylum level.

The bacterial co-occurrence networks were constructed according to species grouped among sites during succession including the early, intermediate, and later stages (Figures 3 and S4 in Supporting Information S1). In these networks, the node numbers varied between 123 and 846, and the link numbers varied between 66 and 1,174, 80% of which were positive links. Compared with the bulk soils, the rhizosheath soils had more nodes and links in the networks, especially at the early and intermediate stages (Figure 3a). At the phylum and class level, Proteobacteria, Acidobacteria, and Planctomycetes dominated the nodes, and the proportion of nodes in different taxa changed significantly with succession (Figures 3b and S4 in Supporting Information S1). Furthermore, the network stability indicated by the natural connectivity decreased at the later stage relative to the early stage (Figure 3c). If random nodes were removed from the network, the connectivity decreased markedly at each stage with a similar range. Meanwhile, the network connectivity was greater at the early stage than at the intermediate and later stages, regardless of whether some nodes were removed or not.

3.3. Bacterial P-Cycling Functional Genes

Based on the quantified absolute gene abundances, we evaluated the succession patterns of P-cycling gene proportion, abundance, and composition during the succession (Figure 4). Among the eight P-cycling functional genes, the P_O-mineralization genes (*phnK*, *phoD*, *bpp* and *phoX*, 80%–91%, mean: 84%) were dominant along the chronosequence in both the rhizosheath and bulk soils, followed by the polyP-hydrolysis gene (*ppx*, 7.2%–15%, 12%), the P_i-solubilization gene (*pqqC*, 0%–8.2%, 4.0%), and then the polyP-biosynthesis gene (*ppk3*, 0%–0.24%, 0.11%) (Figure 4a). A significant difference in the composition of P-cycling genes was observed among succession stages, as indicated by the NMDS analysis (Figure 4b). In general, the absolute abundance of the P-cycling genes was similar in the rhizosheath and bulk soils, except at Stages 3–4 (Figures 4c and S5 in Supporting Information S1). The abundance of the P_O-mineralization and polyP-hydrolysis genes in the rhizosheath soils decreased with increasing succession stage (except at Stage 4), while the abundance in the bulk soils presented a parabolic pattern with succession. Specifically, the gene abundances of P_O mineralization (*phnK*, *phoD*), P_i solubilization, and polyP biosynthesis were greater in the bulk soils at Stage 3 and in the rhizosheath soils at Stage 4.

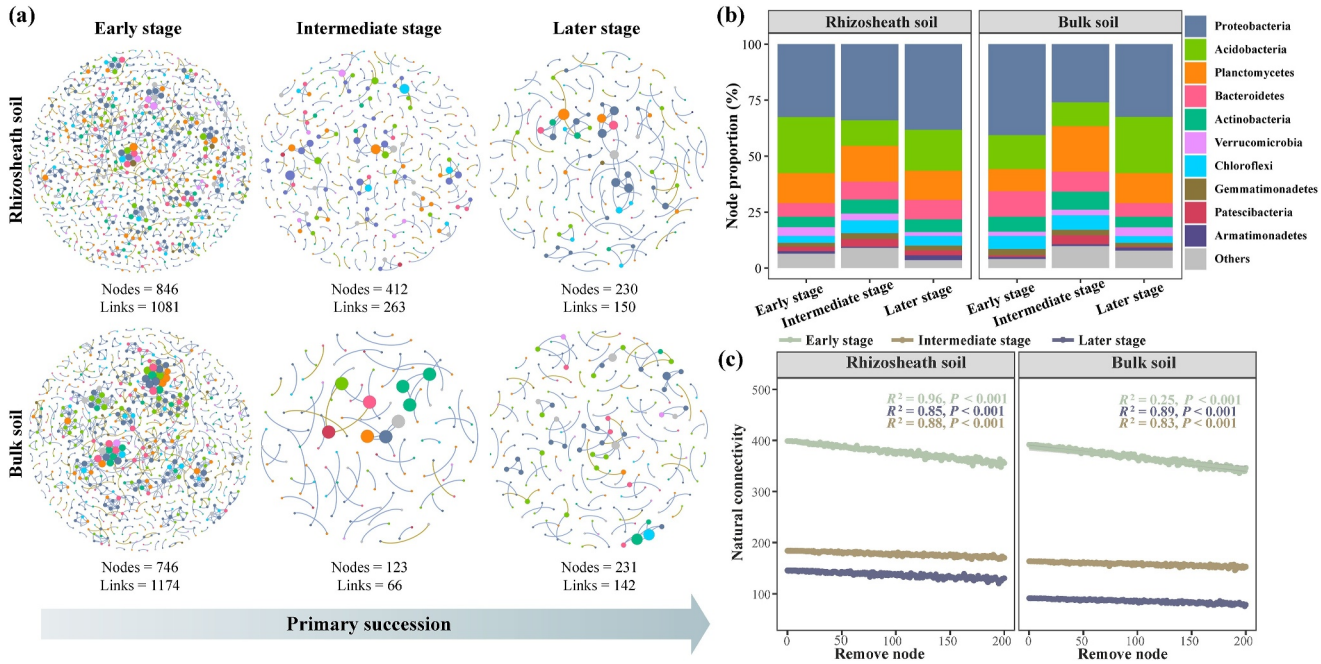

Figure 3. Co-occurrence networks and robustness analysis for bacterial community in the rhizosheath and bulk soils at the early, intermediate and later stages of succession. (a) Co-occurrence patterns of bacterial community. Each node represents a bacterial taxon at the phylum level, and the size of each node is proportional to its number of links. Links of two nodes represent strong ($R > 0.8$) and significant ($P < 0.01$) correlations between bacterial taxa, a blue line represents a positive correlation, and a brown line represents a negative correlation. (b) The proportion of nodes representing different bacterial phyla in each network. (c) Robustness analysis is shown as the relationships between bacteria natural connectivity and the number of removed nodes, and a larger decline at the same number indicates less robustness or stability within the network.

3.4. Correlation of Bacterial Community Structure and P-Cycling Genes With Soil P Fractions

We used the Mantel test to decipher the relationships of bacterial community composition and P-cycling potential (the absolute abundances of P_O-mineralization and polyP-hydrolysis genes) with soil P fractions (Figure 5). In both the rhizosheath and bulk soils, we observed a significant correlation between community composition and soil P fractions, including TP, ASP, P_O, and P_i (Mantel's $P < 0.01$), while P-cycling gene abundances were only significantly correlated with P_O and P_i in the rhizosheath soils (Mantel's $P < 0.05$). Moreover, the abundance of P_O-mineralization gene exhibited a significant correlation with SOC, MBC, and BG + CBH in the rhizosheath soils (Mantel's $P < 0.05$) but not in the bulk soils. The taxa-gene-P networks revealed that soil P fractions were correlated with bacterial taxa rather than P-cycling genes (Figure 6a). In the rhizosheath and bulk soils, the number of both nodes and links in the networks decreased during the succession, and the correlation between bacterial taxa and soil P fractions was stronger in the rhizosheath soils than in the bulk soils (except at the intermediate stage). In addition, we observed a significant correlation between bacterial taxa and P_O at the intermediate and later stages. As indicated by the Random Forest analysis, P_O and bacterial community composition (especially for Actinobacteria, Verrucomicrobia, Acidobacteria, Gammaproteobacteria, Bacteroidia and Deltaproteobacteria) were good predictors of the ASP variation (Figures 6b and 6c). Besides, we found more bacterial taxa associated with P-cycling genes in the bulk soils than in the rhizosheath soils, and the number of links and nodes in the taxa-gene co-occurrence network decreased with succession (Figure S6 in Supporting Information S1). The bacterial community including Proteobacteria, Acidobacteria, and Planctomycetes was closely associated with the genes of P_O mineralization, P_i solubilization, polyP hydrolysis and biosynthesis.

4. Discussion

4.1. Bacterial Community Structure Dominated Soil P Cycling

Supporting our hypotheses, our results showed a closer link between bacterial community composition and soil P fractions in both the rhizosheath and bulk soils than the P-cycling functional genes (Figures 5 and 6). A previous study suggested the importance of bacterial diversity for the biogeochemical cycling of soil nutrients, including P,

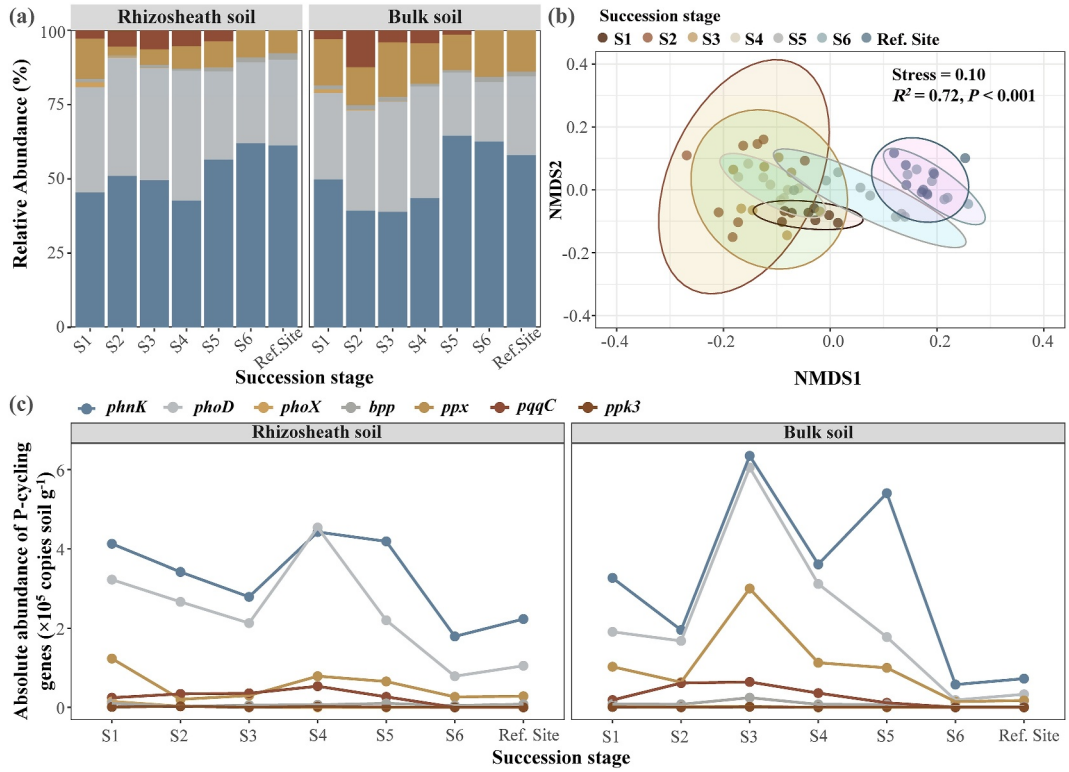

Figure 4. The succession pattern of bacterial phosphorus (P)-cycling functional genes along the chronosequence and at the reference site. (a) Relative proportions of P-cycling genes at different successional stages. (b) Non-metric Multidimensional Scaling (NMDS) analysis of P-cycling genes at different successional stages. (c) Absolute abundances of P-cycling genes.

in plantation ecosystems (Jiao et al., 2018). Our findings further underscore that bacterial community structure, rather than P-cycling functional potential, is a better predictor of soil P cycling in the natural P-rich alpine ecosystems of the eastern Tibetan Plateau. Specifically, bacterial diversity is critical for soil P transformation (Escalas et al., 2019; Luo et al., 2019), and a more diverse and complex bacterial community tends to facilitate P_O mineralization and P_i solubilization.

During the early stages of succession, we observed a significant increase in bacterial diversity and shifts in community composition, which corresponded with a marked decrease in P_i concentration and an increase in P_O concentration (Figures 1 and 2). These patterns suggest that bacteria contribute to P immobilization by facilitating soil P_i solubilization, thereby elevating P_O accumulation in the soils. Contrary to previous studies that link higher microbial diversity and network complexity with enhanced P turnover (Gaiero et al., 2021; Liu et al., 2022), our results indicate an opposite variation trend between bacterial diversity and network complexity at the intermediate stage (Figures 2 and 3). This may be attributed to elevated C and nutrient inputs into soils during vegetation succession (Kardol et al., 2006; Wang et al., 2016), which allow diverse bacterial communities to utilize various nutrient acquisition strategies, reducing the necessity for complex interspecific interactions. As such, the complexity of bacterial networks may serve as a more effective indicator of soil P turnover in P-rich soils. Additionally, we observed a decrease in SOC concentrations with increasing bacterial diversity in bulk soils (Table 1), suggesting that the shift in bacterial diversity from early to intermediate stages may facilitate organic matter mineralization for P demand, potentially diminishing soil C sequestration (Cui et al., 2020; Luo et al., 2022). These findings reveal the crucial role of bacterial communities in driving P transformation during early pedogenesis, emphasizing the need to focus on the dynamics of both dormant and active communities under the rapid changes in soil conditions.

More importantly, our study reveals the critical roles of specific bacterial taxa in soil P cycling during primary succession. We found that Proteobacteria was the most abundant bacterial taxon, serving as core entities in the co-occurrence networks (Figures 2 and 3 and S4 in Supporting Information S1). This finding highlights the

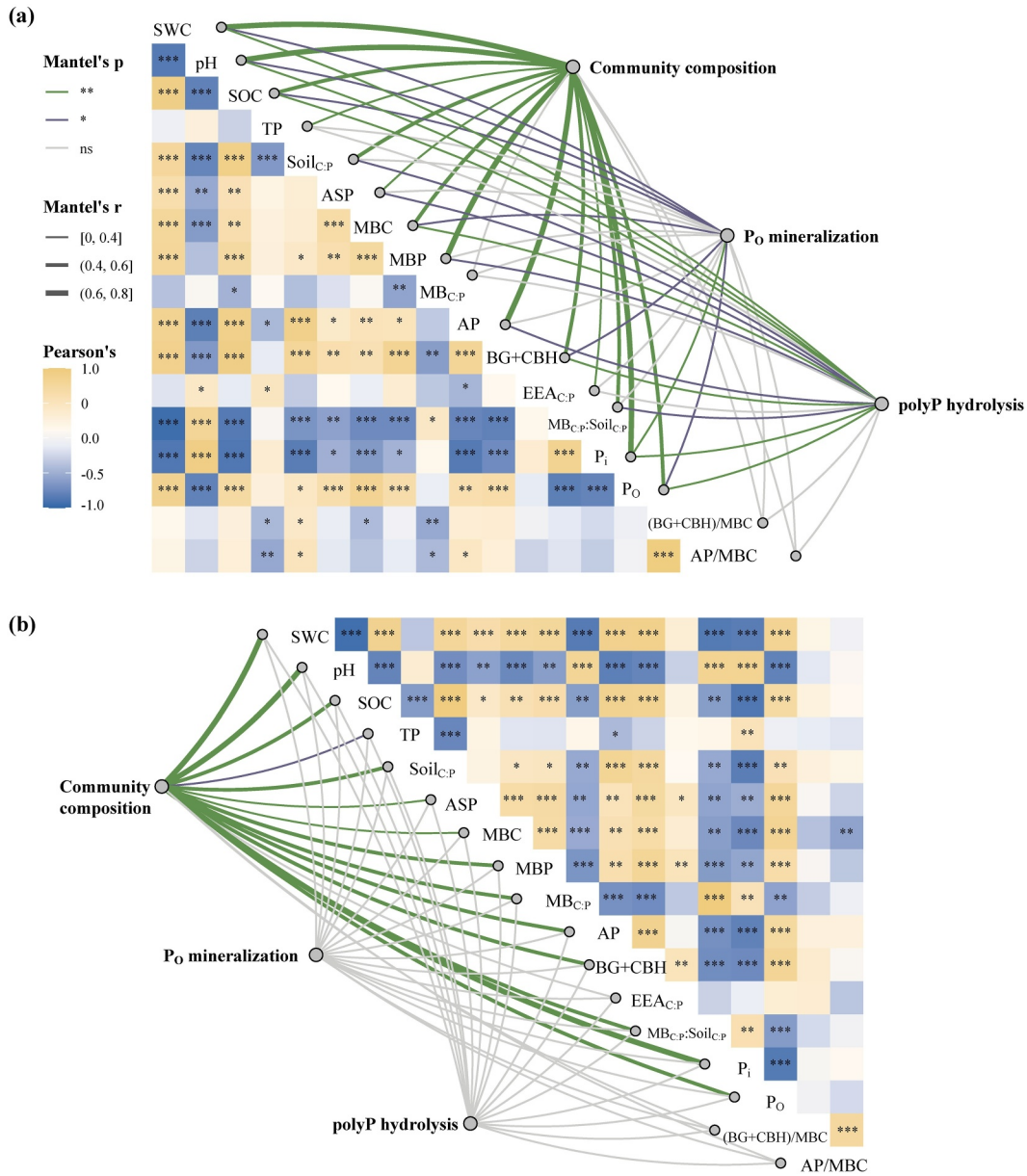

Figure 5. Correlations of bacterial community composition, P_O-mineralization, and polyP-hydrolysis gene abundances with soil physicochemical and biochemical properties in the rhizosheath (a) and bulk (b) soils. SWC: soil water content, SOC: soil organic carbon, TP: total phosphorus, $Soil_{C:P}$: the ratio of SOC to TP, ASP: available soil phosphorus, MBC: microbial biomass carbon, MBP: microbial biomass phosphorus, $MB_{C:P}$: the ratio of MBC to MBP, BG + CBH: the activity of C-acquiring enzymes, AP: the activity of phosphatase, $EEA_{C:P}$: the ratio of (BG + CBH) to AP, P_O mineralization: organic P mineralization, polyP hydrolysis: polyphosphate hydrolysis. *, $P < 0.05$, **, $P < 0.01$, ***, $P < 0.001$.

importance of abundant microbial species in key ecological niches, particularly in their contribution to soil P turnover (Richardson & Simpson, 2011). Proteobacteria, knowing for secreting phosphatases and mineral-solubilizing compounds, are instrumental in promoting soil P availability (Liang et al., 2020; Yao et al., 2018). Moreover, bacterial taxa with a relative abundance of >1% were strong predictors of soil available P (Figure 6c), reinforcing the importance of abundant bacterial taxa for P cycling processes. In addition to Proteobacteria, Actinobacteria and Bacteroidetes, both of which harbor functional genes like *phoD* and *phoX*, were identified as key players in soil P cycling (Bai et al., 2020; Liang et al., 2020). Actinobacteria, known for their correlation with soil P availability, and Bacteroidetes, which can express high functional potential for P_O mineralization in response to P_i depletion, were also central to P cycling (Bai et al., 2020; Lidbury et al., 2022;

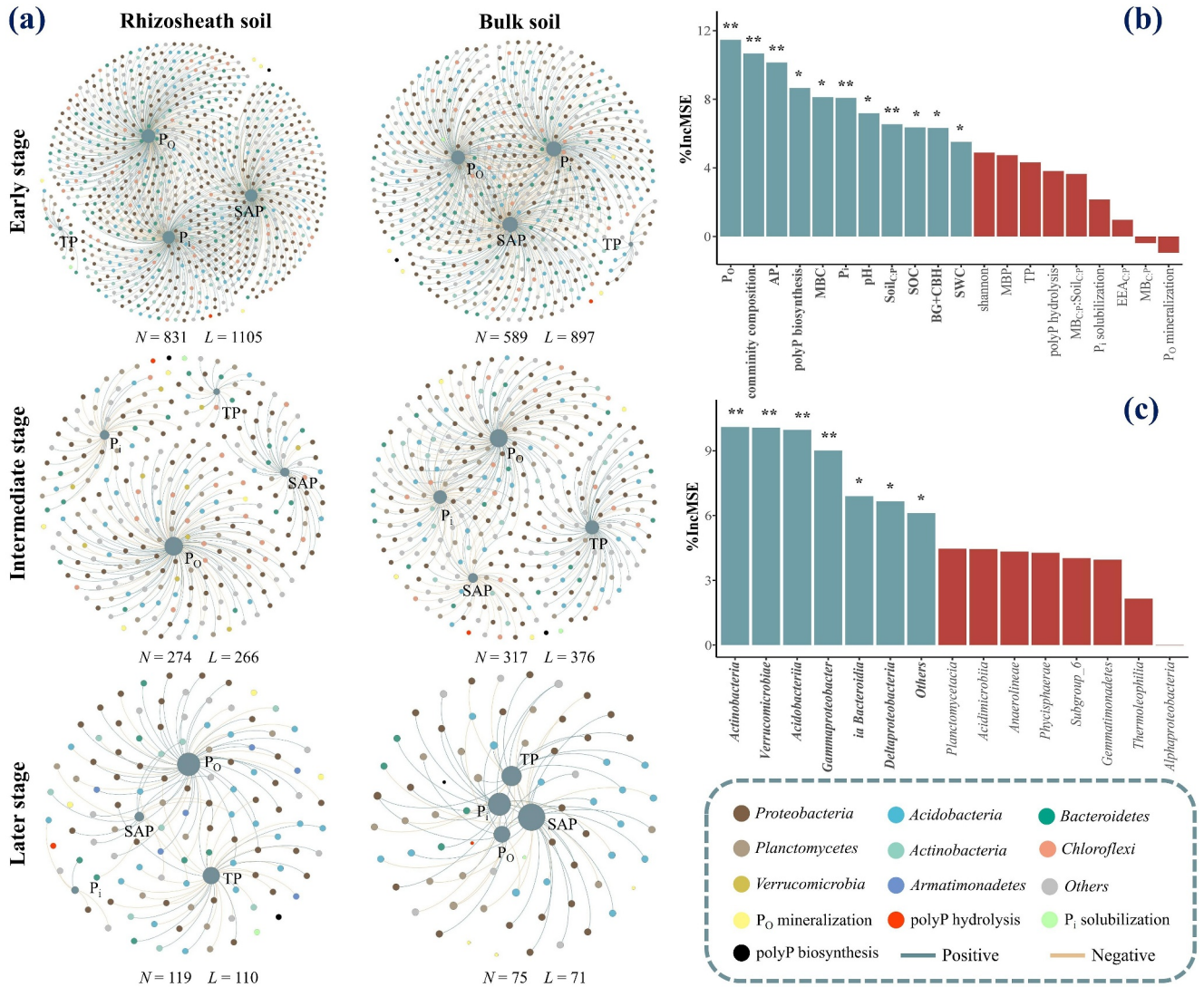

Figure 6. The visualization of the co-occurrence networks of bacterial community and phosphorus (P)-cycling genes with soil P fractions and the potential drivers in available soil P during primary succession. (a) Taxa-gene-P networks in the rhizosheath and bulk soils at the early, intermediate and later stages. The size of each node is proportional to its number of links. Links of two nodes represent strong ($R > 0.8$) and significant ($P < 0.05$) correlations between bacterial taxa, P-cycling gene, and soil P fractions. A blue line represents a positive correlation, and a yellow line represents a negative correlation. N: nodes, L: links. (b) The importance (percent of increase in mean square error) of soil properties, bacterial community composition and P-cycling genes in ASP variation was determined by random forest (RF) analysis. (c) The importance of bacterial abundant classes (>1% of total community) as drivers for ASP variation by RF analysis. The importance of each predictor was evaluated by the increase in mean squared error (MSE), with higher MSE% values implying more important variables. The asterisks and bold font indicate that the predictor was significant (*, $P < 0.05$; **, $P < 0.01$); blue columns denote significant factors whereas red ones are not. SWC: soil water content, SOC: soil organic carbon, TP: total phosphorus, $Soil_{C:P}$: the ratio of SOC to TP, ASP: available soil phosphorus, MBC: microbial biomass carbon, MBP: microbial biomass phosphorus, $MB_{C:P}$: the ratio of MBC to MBP, BG + CBH: the activity of C-acquiring enzymes, AP: the activity of phosphatase, $EEA_{C:P}$: the ratio of (BG + CBH) to AP, P_O mineralization: organic P mineralization, polyP hydrolysis: polyphosphate hydrolysis. *, $P < 0.05$, **, $P < 0.01$.

Luo et al., 2019). These findings align with previous studies that emphasize the role of abundant microbial species in resource competition and nutrient cycling (Chen et al., 2020; Liu et al., 2022). However, our study expands on this by demonstrating the specific contributions of Proteobacteria, Bacteroidetes, and Actinobacteria to soil P turnover through their functional genes (e.g., *phnK*, *phoD*, and *phoX*, Figure S6 in Supporting Information S1). In summary, the results of the present study highlight the significance of bacterial diversity, interspecific interactions, and the roles of abundant and functionally important taxa in driving soil P cycling during primary succession.

4.2. Bacteria-Mediated Soil P Cycling Determined by Carbon Demand

This finding contrasts with previous studies by Oliverio et al. (2020) and Wu et al. (2022). Typically, it is assumed that an increase in the abundance of P-cycling functional genes would enhance soil P availability under P-limited conditions (Dai et al., 2020; Liang et al., 2020). However, the results of the present study provide compelling evidence that variations in bacterial P functional genes do not necessarily drive changes in soil P fractions during primary succession. It is possible that bacterial communities constitutively express P-cycling genes during organic matter mineralization, even when limited by other soil resources (Brankatschk et al., 2011; Wang, Wu, et al., 2021). This notion is supported by the ratios of $MB_{C:P}$, which were approximately 100 across all stages except the bulk soils at Stage 1 (Figure S3 in Supporting Information S1). This implies that microbial P_O mineralization may be driven by microbial C acquisition rather than stoichiometric imbalance in the soils (McConnell et al., 2020). Meanwhile, the ratios of $EEA_{C:P}$ were greater than 1, indicating that microbes may be more limited by C than by P. Consequently, soil microbes may degrade phosphorylated organic compounds to meet their C demand, while releasing available P to the soils as a byproduct (Spohn & Kuzyakov, 2013). This interpretation suggests that the abundances of genes involved in P_O mineralization and polyP hydrolysis are functionally linked to both SOC and P fractions, reflecting microbial C demand.

Notably, our study revealed a high prevalence of the gene encoding the C-P lyase subunit, *phnK*, throughout the chronosequence (Figure 4), suggesting a significant bacterial potential to cleave C-P bonds despite the associated high energy costs (Kamat et al., 2011). Given the ample substrate P in the soils examined, it is unexpected that bacteria would invest considerable energy to produce the C-P lyase enzyme for P acquisition (Wang et al., 2020). Thus, the high abundance of *phnK* suggests that bacterial communities may enhance phosphonate utilization primarily to access C resources (Manav et al., 2018; Metcalf & van der Donk, 2009). This notion is supported by our observation of a significant decrease in MBC concentrations concurrent with an increase in the abundance of *phnK* in the bulk soils at Stages 3–4 (Figures 4 and S3 in Supporting Information S1). Moreover, polyP, a crucial energy and phosphate reserve within microbial cells, is known to enhance microbial survival under P scarcity (Albi & Serrano, 2016). We found that the abundance of the polyP hydrolysis gene (*ppx*), followed by P_O-mineralization genes, was tightly linked to SOC rather than soil P fractions (Figures 4 and 5). This suggests that bacteria may degrade polyP polymers as an energy donor for C acquisition, particularly under conditions of C-deficiency by promoting polyP hydrolysis (Mason-Jones et al., 2022). Our findings, from the functional perspective, indicate that P_O mineralization in the P-rich alpine soils is probably driven by biological mineralization processes rather than biochemical processes. Specifically, bacteria-mediated P_O mineralization and polyP hydrolysis are determined by bacterial C demand during the mineralization of soil organic matter (McConnell et al., 2020).

4.3. Importance of Bacteria in Soil P Cycling During Primary Succession

Our study demonstrates that bacterial community structure determines soil P turnover along the chronosequence at the glacier forefield, initiating P cycling during the early stages of succession (Figure 7), in alignment with our hypothesis. Given the limited colonization by plants and fungi at these early stages, bacteria emerge as the primary pioneer colonizers, accessing scarce soil resources (Bardgett et al., 2007; Reichert et al., 2022). Consequently, bacteria initiate crucial biogeochemical processes for ecosystem establishment and nutrient transformation by utilizing the ancient and recalcitrant organic matter from the glacier forefield as substrates (Hood et al., 2015; Ni et al., 2023). The influence of bacterial community structure on soil P cycling at an early stage can be explained by several potential mechanisms, two of which we propose here. First, under low organic matter content at the early stage, stochastic processes may drive the bacterial community establishment, leading to the formation of a functionally stable community (Dini-Andreote et al., 2015; Yu et al., 2023). Core taxa in the bacterial network, such as fast-growing Proteobacteria, Actinobacteria, and Bacteroidetes, can expand rapidly (Fierer et al., 2007; Zhou et al., 2019), initially promoting P_i solubilization and P_O accumulation, as evidenced by shifts in soil P fractions and P-cycling gene abundances (Figures 1 and 4). Additionally, the dominance of N_2-fixing bacteria and their symbiotic relationships with plants at the early stage can stimulate soil P cycling along with increasing N contents (Benavent-González et al., 2019; Bergkemper et al., 2016). This is confirmed by the significant increase in available soil P concentration and the decrease in P_i concentration at the early stage (Figure 1). Second, a diverse bacterial community, comprising taxa with complementary functions, displays a strong potential to solubilize mineral phosphates and mineralize various P_O fractions in the soils. This exemplifies microbial functional redundancy, which in turn enhances the efficiency of P cycling (Escalas et al., 2019; Louca

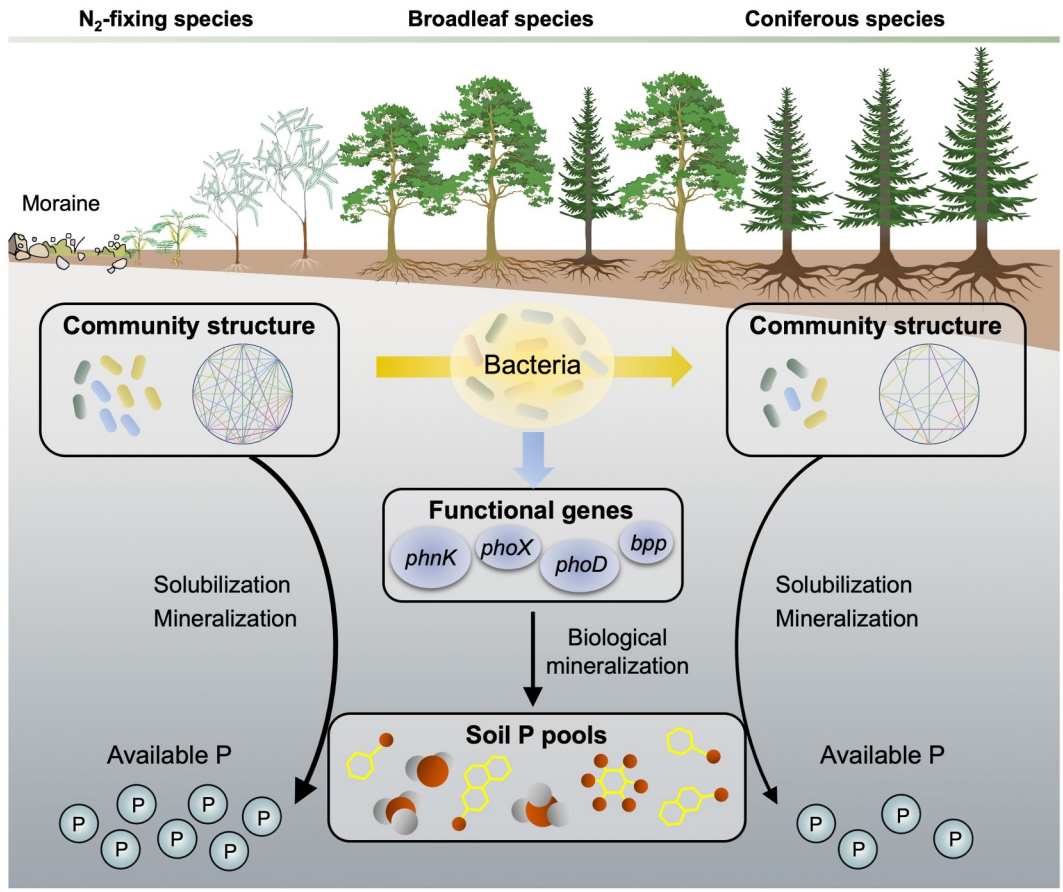

Figure 7. Mechanisms of the bacteria-mediated phosphorous transformation along the chronosequence at the glacier forefield. Bacterial diversity, taxa abundance, and interspecific interactions modulate soil phosphorous fractions across different successional stages. Bacterial phosphorus-cycling functional genes, primarily driven by their carbon demand, regulate soil phosphorous turnover via the biological mineralization process. During the early stages of ecosystem succession, bacteria play a crucial role in driving soil P turnover and enhancing P availability, while their influence diminishes significantly with vegetation succession.

et al., 2018). This concept is supported by the observed increase in bacterial diversity and the higher abundances of P-cycling functional genes involved in P_O mineralization and P_i solubilization at the early stage (Figures 2 and 4, Figure S5 in Supporting Information S1).

Our findings reveal a decline in bacterial influence on soil P cycling as the succession advances, characterized by reduced taxa-gene-P network complexity, with bacterial diversity and P-cycling gene abundances peaking at the intermediate stages but decreasing thereafter (Figure 7). This pattern aligns with the intermediate disturbance hypothesis (Ortiz-Álvarez et al., 2018; Zhang et al., 2018), where maximum bacterial diversity and P-cycling functional potential occur during transitional stages dominated by deciduous forests, which create a heterogeneous soil environment, including diverse P fractions, conducive to species coexistence (Kardol et al., 2006; Wu et al., 2019). Primary succession theory proposes that soil P cycling becomes more closed at later succession stages, with a reduction in available P and an increase in the refractory P_O fraction (Lang et al., 2016; Oliverio et al., 2020). This means that bacteria exhibit a reduced capacity for P_O turnover at later stages, where fungal communities predominate ecological niches and potentially mineralize P_O by secreting phosphatases (He et al., 2020; Reichert et al., 2022). Notably, environmental stresses such as soil acidification and nutrient deficiency at later stages further constrain bacterial P-cycling functions, as indicated by changes in bacterial community composition and the prevalence of Acidobacteria (Figure 2). These stressors, coupled with the increasing dominance of plants and mycorrhizal associations in P acquisition, diminish the bacterial contribution to soil P cycling, as evidenced by the abundance of P-cycling genes (Figure 4). Our findings also highlight the stability of available P in rhizosheath soils during later succession stages, suggesting that plants have evolved diverse

P-acquisition strategies such as root expansion, carboxylate release, and mycorrhizal symbioses to maintain soil P availability (Chen et al., 2020; Lambers, 2022). With the ongoing retreat of alpine glaciers under global warming, bacteria play a pivotal role in enhancing soil P availability, advancing plant colonization and succession, and potentially contributing to ecosystem C storage (Li et al., 2024). Future studies should focus on bacterial contributions to soil P turnover and comprehensively elucidate bacteria-mediated P cycling dynamics in rapidly changing alpine ecosystems.

5. Conclusions

Our findings provide evidence that the bacterial community structure plays a vital role in initiating soil P cycling following glacial retreat. The high potential of bacteria for P_O mineralization regardless of succession stages in P-rich alpine soils may be more the result of bacterial C demand than P demand. These findings, from the functional perspective, advance the concept that P_O mineralization in P-rich soils is a process of dual element (C and P) biological mineralization. Furthermore, the abundant and functional components of bacterial taxonomy mainly governed soil P turnover, although their capability to mobilize P declined with soil P depletion. In the context of intensifying global warming and anthropogenic disturbance, this study has important implications for understanding the roles of the bacterial community in early ecological succession and for managing microbial resources to restore P-rich degraded ecosystems. Moreover, the findings emphasize the critical importance of directing attention toward microbial-mediated coupled C and P dynamics in emerging ecosystems following glacier retreat, which may expedite the degradation of soil organic matter in the glacier forefields worldwide.

Data Availability Statement

The raw sequences for bacteria are available in the National Center for Biotechnology Information (NCBI) Sequence Read Archive under project ID PRJNA814341, and other source data and R code used for data analysis in this study are archived in the publicly accessible repository Zenodo (Wang et al., 2024).

Acknowledgments
This work was supported by the Joint Funds of the National Natural Science Foundation of China (U21A20237), the Science and Technology Research Program of Institute of Mountain Hazards and Environment, Chinese Academy of Sciences (IMHE-ZYTS-07, IMHE-ZDRW-06), and the National Natural Science Foundation of China (41977031, 42271064), and PBR was supported by the U.S. National Science Foundation, Biological Integration Institutes Grant NSF-DBI-2021898.

References

Albi, T., & Serrano, A. (2016). Inorganic polyphosphate in the microbial world. Emerging roles for a multifaceted biopolymer. *World Journal of Microbiology and Biotechnology*, *32*(2), 1–12. https://doi.org/10.1007/s11274-015-1983-2

Bai, Y., Xiang, Q. J., Zhao, K., Yu, X. M., Chen, Q., Ma, M. G., et al. (2020). Plant and soil development cooperatively shaped the composition of the *phoD*-harboring bacterial community along the primary succession in the Hailuogou Glacier Chronosequence. *mSystems*, *5*(4), 004755-20. https://doi.org/10.1128/msystems.00475-20

Bardgett, R. D., Richter, A., Bol, R., Garnett, M. H., Bäumler, R., Xu, X. L., et al. (2007). Heterotrophic microbial communities use ancient carbon following glacial retreat. *Biology Letters*, *3*(5), 487–490. https://doi.org/10.1098/rsbl.2007.0242

Benavent-González, A., Raggio, J., Villagra, J., Blanquer, J. M., Pintado, A., Rozzi, R., et al. (2019). High nitrogen contribution by Gunnera magellanica and nitrogen transfer by mycorrhizas drive an extraordinarily fast primary succession in sub-Antarctic Chile. *New Phytologist*, *223*(2), 661–674. https://doi.org/10.1111/nph.15838

Benjamini, Y., & Hochberg, Y. (1995). Controlling the false discovery rate: A practical and powerful approach to multiple testing. *Journal of the Royal Statistical Society: Series B*, *57*(1), 289–300. https://doi.org/10.1111/j.2517-6161.1995.tb02031.x

Bergkemper, F., Schoeler, A., Engel, M., Lang, F., Krueger, J., Schloter, M., & Schulz, S. (2016). Phosphorus depletion in forest soils shapes bacterial communities towards phosphorus recycling systems. *Environmental Microbiology*, *18*(6), 1988–2000. https://doi.org/10.1111/1462-2920.13188

Bosson, J. B., Huss, M., Cauvy-Fraunié, S., Clément, J. C., Costes, G., Fischer, M., et al. (2023). Future emergence of new ecosystems caused by glacial retreat. *Nature*, *620*(7974), 562–569. https://doi.org/10.1038/s41586-023-06302-2

Brankatschk, R., Töwe, S., Kleineidam, K., Schloter, M., & Zeyer, J. (2011). Abundances and potential activities of nitrogen cycling microbial communities along a chronosequence of a glacier forefield. *The ISME Journal*, *5*(6), 1025–1037. https://doi.org/10.1038/ismej.2010.184

Brookes, P. C., Powlson, D. S., & Jenkinson, D. S. (1982). Measurement of microbial biomass phosphorus in soil. *Soil Biology and Biochemistry*, *14*(4), 319–329. https://doi.org/10.1016/0038-0717(82)90001-3

Chen, Y., Sun, R. B., Sun, T. T., Chen, P., Yu, Z. Y., Ding, L. Y., et al. (2020). Evidence for involvement of keystone fungal taxa in organic phosphorus mineralization in subtropical soil and the impact of labile carbon. *Soil Biology and Biochemistry*, *148*, 107900. https://doi.org/10.1016/j.soilbio.2020.107900

Cui, Y. X., Bing, H. J., Fang, L. C., Jiang, M., Shen, G. T., Yu, J. L., et al. (2019). Extracellular enzyme stoichiometry reveals the carbon and phosphorus limitations of microbial metabolisms in the rhizosphere and bulk soils in alpine ecosystems. *Plant and Soil*, *458*(1–2), 1–14. https://doi.org/10.1007/s11104-019-04159-x

Cui, Y. X., Wang, X., Zhang, X. C., Ju, W. L., Duan, C. J., Guo, X. B., et al. (2020). Soil moisture mediates microbial carbon and phosphorus metabolism during vegetation succession in a semiarid region. *Soil Biology and Biochemistry*, *147*, 107814. https://doi.org/10.1016/j.soilbio.2020.107814

Dai, Z. M., Liu, G. F., Chen, H. H., Chen, C. R., Wang, J. K., Ai, S. Y., et al. (2020). Long-term nutrient inputs shift soil microbial functional profiles of phosphorus cycling in diverse agroecosystems. *The ISME Journal*, *14*(3), 757–770. https://doi.org/10.1038/s41396-019-0567-9

Darcy, J. L., Schmidt, S. K., Knelman, J. E., Cleveland, C. C., Castle, S. C., & Nemergut, D. R. (2018). Phosphorus, not nitrogen, limits plants and microbial primary producers following glacial retreat. *Science Advances*, *4*(5), eaaq0942. https://doi.org/10.1126/sciadv.aaq0942

Deng, Y., Jiang, Y. H., Yang, Y. F., He, Z. L., Luo, F., & Zhou, J. Z. (2012). Molecular ecological network analyses. *BMC Bioinformatics*, *13*, 1–20. https://doi.org/10.1186/1471-2105-13-113

Dini-Andreote, F., Stegen, J. C., van Elsas, J. D., & Salles, J. F. (2015). Disentangling mechanisms that mediate the balance between stochastic and deterministic processes in microbial succession. *Proceedings of the National Academy of Sciences of the United States of America*, *112*(11), E1326–E1332. https://doi.org/10.1073/pnas.1414261112

Elser, J. J., Bracken, M. E. S., Cleland, E. E., Gruner, D. S., Harpole, W. S., Hillebrand, H., et al. (2007). Global analysis of nitrogen and phosphorus limitation of primary producers in freshwater, marine and terrestrial ecosystems. *Ecology Letters*, *10*(12), 1135–1142. https://doi.org/10.1111/j.1461-0248.2007.01113.x

Escalas, A., Hale, L., Voordeckers, J. W., Yang, Y. F., Firestone, M. K., Alvarez-Cohen, L., & Zhou, J. Z. (2019). Microbial functional diversity: From concepts to applications. *Ecology and Evolution*, *9*(20), 12000–12016. https://doi.org/10.1002/ece3.5670

Ficetola, G. F., Marta, S., Guerrieri, A., Cantera, I., Bonin, A., Cauvy-Fraunié, S., et al. (2024). The development of terrestrial ecosystems emerging after glacier retreat. *Nature*, *632*(8024), 336–342. https://doi.org/10.1038/s41586-024-07778-2

Ficetola, G. F., Marta, S., Guerrieri, A., Gobbi, M., Ambrosini, R., Fontaneto, D., et al. (2021). Dynamics of ecological communities following current retreat of glaciers. *Annual Review of Ecology Evolution and Systematics*, *52*(1), 405–426. https://doi.org/10.1146/annurev-ecolsys-010521-040017

Fierer, N., Bradford, M. A., & Jackson, R. B. (2007). Toward an ecological classification of soil bacteria. *Ecology*, *88*(6), 1354–1364. https://doi.org/10.1890/05-1839

Gaiero, J. R., Tosi, M., Bent, E., Boitt, G., Khosla, K., Turner, B. L., et al. (2021). Soil microbial communities influencing organic phosphorus mineralization in a coastal dune chronosequence in New Zealand. *FEMS Microbiology Ecology*, *97*(4), fiab034. https://doi.org/10.1093/femsec/fiab034

He, Q. Q., Wu, Y. H., Bing, H. J., Zhou, J. Z., & Wang, J. P. (2020). Vegetation type rather than climate modulates the variation in soil enzyme activities and stoichiometry in subalpine forests in the eastern Tibetan Plateau. *Geoderma*, *374*, 114424. https://doi.org/10.1016/j.geoderma.2020.114424

Heuck, C., Weig, A., & Spohn, M. (2015). Soil microbial biomass C:N:P stoichiometry and microbial use of organic phosphorus. *Soil Biology and Biochemistry*, *85*, 119–129. https://doi.org/10.1016/j.soilbio.2015.02.029

Hood, E., Battin, T. J., Fellman, J., O'Neel, H., & Spencer, R. G. (2015). Storage and release of organic carbon from glaciers and ice sheets. *Nature Geoscience*, *8*(2), 91–96. https://doi.org/10.1038/ngeo2331

Jiao, S., Chen, W. M., Wang, J. L., Du, N. N., Li, Q. P., & Wei, G. H. (2018). Soil microbiomes with distinct assemblies through vertical soil profiles drive the cycling of multiple nutrients in reforested ecosystems. *Microbiome*, *6*, 1–13. https://doi.org/10.1186/s40168-018-0526-0

Joergensen, R. G. (1996). The fumigation-extraction method to estimate soil microbial biomass: Calibration of the k_{EC} value. *Soil Biology and Biochemistry*, *28*(1), 25–31. https://doi.org/10.1016/0038-0717(95)00102-6

Kamat, S. S., Williams, H. J., & Raushel, F. M. (2011). Intermediates in the transformation of phosphonates to phosphate by bacteria. *Nature*, *480*(7378), 570–573. https://doi.org/10.1038/nature10622

Kardol, P., Martijn Bezemer, T., & van der Putten, W. H. (2006). Temporal variation in plant-soil feedback controls succession. *Ecology Letters*, *9*, 1080–1088. https://doi.org/10.1111/j.1461-0248.2006.00953.x

Laliberté, E., Turner, B. L., Costes, T., Pearse, S. J., Wyrwoll, K. H., Zemunik, G., & Lambers, H. (2012). Experimental assessment of nutrient limitation along a 2-million-year dune chronosequence in the south-western Australia biodiversity hotspot. *Journal of Ecology*, *100*(3), 631–642. https://doi.org/10.1111/j.1365-2745.2012.01962.x

Lambers, H. (2022). Phosphorus acquisition and utilization in plants. *Annual Review of Plant Biology*, *73*(1), 17–42. https://doi.org/10.1146/annurev-arplant-102720-125738

Lang, F., Bauhus, J., Frossard, E., George, E., Kaiser, K., Kaupenjohann, M., et al. (2016). Phosphorus in forest ecosystems: New insights from an ecosystem nutrition perspective. *Journal of Plant Nutrition and Soil Science*, *179*(2), 129–135. https://doi.org/10.1002/jpln.201500541

Li, H. Z., Peng, J. J., Yang, K., Zhang, Y. Y., Chen, Q. L., Zhu, Y. G., & Cui, L. (2024). Single-cell exploration of active phosphate-solubilizing bacteria across diverse soil matrices for sustainable phosphorus management. *Nature Food*, *5*(8), 1–11. https://doi.org/10.1038/s43016-024-01024-8

Li, X., & Xiong, S. F. (1995). Vegetation primary succession on glacier foreland in Hailuogou, Mt. Gongga. *Mountain Research*, *12*, 109–115.

Liang, J. L., Liu, J., Jia, P., Yang, T. T., Zeng, Q. W., Zhang, S. C., et al. (2020). Novel phosphate-solubilizing bacteria enhance soil phosphorus cycling following ecological restoration of land degraded by mining. *The ISME Journal*, *14*(6), 1600–1613. https://doi.org/10.1038/s41396-020-0632-4

Lidbury, I. D., Scanlan, D. J., Murphy, A. R., Christie-Oleza, J. A., Aguilo-Ferretjans, M. M., Hitchcock, A., & Daniell, T. J. (2022). A widely distributed phosphate-insensitive phosphatase presents a route for rapid organophosphorus remineralization in the biosphere. *Proceedings of the National Academy of Sciences*, *119*(5), e2118122119. https://doi.org/10.1073/pnas.2118122119

Liu, X. P., Wang, H. T., Wu, Y. J., Bi, Q. F., Ding, K., & Lin, X. Y. (2022). Manure application effects on subsoils: Abundant taxa initiate the diversity reduction of rare bacteria and community functional alterations. *Soil Biology and Biochemistry*, *174*, 108816. https://doi.org/10.1016/j.soilbio.2022.108816

Louca, S., Polz, M. F., Mazel, F., Albright, M. B., Huber, J. A., O'Connor, M. I., et al. (2018). Function and functional redundancy in microbial systems. *Nature Ecology and Evolution*, *2*(6), 936–943. https://doi.org/10.1038/s41559-018-0519-1

Luo, G. W., Sun, B., Li, L., Li, M. H., Liu, M. Q., Zhu, Y. Y., et al. (2019). Understanding how long-term organic amendments increase soil phosphatase activities: Insight into *phoD*- and *phoC*-harboring functional microbial populations. *Soil Biology and Biochemistry*, *139*, 107632. https://doi.org/10.1016/j.soilbio.2019.107632

Luo, R. Y., Kuzyakov, Y., Zhu, B., Qiang, W., Zhang, Y., & Pang, X. Y. (2022). Phosphorus addition decreases plant lignin but increases microbial necromass contribution to soil organic carbon in a subalpine forest. *Global Change Biology*, *28*(13), 4194–4210. https://doi.org/10.1111/gcb.16205

Manav, M. C., Sofos, N., Hove-Jensen, B., & Brodersen, D. E. (2018). The Abc of phosphonate breakdown: A mechanism for bacterial survival. *BioEssays*, *40*(11), 1800091. https://doi.org/10.1002/bies.201800091

Mason-Jones, K., Robinson, S. L., Veen, G. F., Manzoni, S., & van der Putten, W. H. (2022). Microbial storage and its implications for soil ecology. *The ISME Journal*, *16*(3), 617–629. https://doi.org/10.1038/s41396-021-01110-w

McConnell, C. A., Kaye, J. P., & Kemanian, A. R. (2020). Reviews and syntheses: Ironing out wrinkles in the soil phosphorus cycling paradigm. *Biogeosciences*, *17*(21), 5309–5333. https://doi.org/10.5194/bg-17-5309-2020

Metcalf, W. W., & van der Donk, W. A. (2009). Biosynthesis of phosphonic and phosphinic acid natural products. *Annual Review of Biochemistry*, *78*(1), 65–94. https://doi.org/10.1146/annurev.biochem.78.091707.100215

Ni, G., Lappan, R., Hernández, M., Santini, T., Tomkins, A. G., & Greening, C. (2023). Functional basis of primary succession: Traits of the pioneer microbes. *Environmental Microbiology*, *25*(1), 171–176. https://doi.org/10.1111/1462-2920.16266

Oliverio, A. M., Bissett, A., McGuire, K., Saltonstall, K., Turner, B. L., & Fierer, N. (2020). The role of phosphorus limitation in shaping soil bacterial communities and their metabolic capabilities. *mBio*, *11*(5). e01718-20. https://doi.org/10.1128/mbio.01718-20

Ortiz-Álvarez, R., Fierer, N., de los Ríos, A., Casamayor, E. O., & Barberán, A. (2018). Consistent changes in the taxonomic structure and functional attributes of bacterial communities during primary succession. *The ISME Jorunal*, *12*(7), 1658–1667. https://doi.org/10.1038/s41396-018-0076-2

Qiu, T. Y., Peñuelas, J., Chen, Y. L., Sardans, J., Yu, J. L., Xu, Z., et al. (2024). Arbuscular mycorrhizal fungal interactions bridge the support of root-associated microbiota for slope multifunctionality in an erosion-prone ecosystem. *iMeta*, *e187*(3). https://doi.org/10.1002/imt2.187

Reichert, T., Rammig, A., Fuchslueger, L., Lugli, L. F., Quesada, C. A., & Fleischer, K. (2022). Plant phosphorus-use and -acquisition strategies in Amazonia. *New Phytologist*, *234*(4), 1126–1143. https://doi.org/10.1111/nph.17985

Richardson, A. E., & Simpson, R. J. (2011). Soil microorganisms mediating phosphorus availability. *Plant Physiology*, *156*(3), 989–996. https://doi.org/10.1104/pp.111.175448

Siles, J. A., Starke, R., Martinovic, T., Fernandes, M., Orgiazzi, A., & Bastida, F. (2022). Distribution of phosphorus cycling genes across land uses and microbial taxonomic groups based on metagenome and genome mining. *Soil Biology and Biochemistry*, *174*, 108826. https://doi.org/10.1016/j.soilbio.2022.108826

Spohn, M., & Kuzyakov, Y. (2013). Phosphorus mineralization can be driven by microbial need for carbon. *Soil Biology and Biochemistry*, *61*, 69–75. https://doi.org/10.1016/j.soilbio.2013.02.013

Vance, E. D., Brookes, P. C., & Jenkinson, D. S. (1987). An extraction method for measuring soil microbial biomass C. *Soil Biology and Biochemistry*, *19*(6), 703–707. https://doi.org/10.1016/0038-0717(87)90052-6

van der heijden, M., Bardgett, R. D., & van Straalen, N. M. (2008). The unseen majority: Soil microbes as drivers of plant diversity and productivity in terrestrial ecosystems. *Ecology Letters*, *11*(3), 296–310. https://doi.org/10.1111/j.1461-0248.2007.01139.x

Walker, T. W., & Syers, J. K. (1976). The fate of phosphorus during pedogenesis. *Geoderma*, *15*, 1–19. https://doi.org/10.1016/0016-7061(76)90066-5

Wang, H. L., Bu, L. Y., Song, F. Q., Tian, J., & Wei, G. H. (2021). Soil available nitrogen and phosphorus affected by functional bacterial community composition and diversity as ecological restoration progressed. *Land Degradation & Development*, *32*(1), 183–198. https://doi.org/10.1002/ldr.3707

Wang, J. P., Wu, Y. H., Li, J. J., He, Q. Q., & Bing, H. J. (2021). Soil enzyme stoichiometry is tightly linked to microbial community composition in successional ecosystems after glacier retreat. *Soil Biology and Biochemistry*, *162*, 108429. https://doi.org/10.1016/j.soilbio.2021.108429

Wang, J. P., Wu, Y. H., Zhou, J., Bing, H. J., & Sun, H. Y. (2016). Carbon demand drives microbial mineralization of organic phosphorus during the early stage of soil development. *Biology and Fertility of Soils*, *52*(6), 825–839. https://doi.org/10.1007/s00374-016-1123-7

Wang, J. P., Wu, Y. H., Zhou, J., Bing, H. J., Sun, H. Y., He, Q. Q., et al. (2020). Soil microbes become a major pool of biological phosphorus during the early stage of soil development with little evidence of competition for phosphorus with plants. *Plant and Soil*, *446*(1–2), 259–274. https://doi.org/10.1007/s11104-019-04329-x

Wang, Y. H., Bing, H. J., Daryl, L. M., Hou, E. Q., Wu, Y. H., Wang, J. P., et al. (2024). Data and code for: Bacterial community structure modulates soil phosphorus turnover at early stages of primary succession [Dataset]. *Zenodo*. https://doi.org/10.5281/zenodo.13690183

Wu, H. L., Xiang, W. H., Ouyang, S., Forrester, D. I., Zhou, B., Chen, L. X., et al. (2019). Linkage between tree species richness and soil microbial diversity improves phosphorus bioavailability. *Functional Ecology*, *33*(8), 1549–1560. https://doi.org/10.1111/1365-2435.13355

Wu, X. J., Rensing, C., Han, D. F., Xiao, K. Q., Dai, Y. X., Tang, Z. X., et al. (2022). Genome-resolved metagenomics reveals distinct phosphorus acquisition strategies between soil microbiomes. *mSystems*, *7*(1). e01107-01121. https://doi.org/10.1128/msystems.01107-21

Xu, L., Cao, H. L., Li, C. N., Wang, C. H., He, N. P., Hu, S. Y., et al. (2022). The importance of rare versus abundant *phoD*-harboring subcommunities in driving soil alkaline phosphatase activity and available P content in Chinese steppe ecosystems. *Soil Biology and Biochemistry*, *164*, 108491. https://doi.org/10.1016/j.soilbio.2021.108491

Yao, Q. M., Li, Z., Song, Y., Wright, S. J., Guo, X., Tringe, S. G., et al. (2018). Community proteogenomics reveals the systemic impact of phosphorus availability on microbial functions in tropical soil. *Nature Ecology and Evolution*, *2*(3), 499–509. https://doi.org/10.1038/s41559-017-0463-5

Yu, S. Y., Lv, J. T., Jiang, L., Geng, P. Y., Cao, D., & Wang, Y. W. (2023). Changes of soil dissolved organic matter and its relationship with microbial community along the Hailuogou glacier forefield chronosequence. *Environmental Science and Technology*, *57*(9), 4027–4038. https://doi.org/10.1021/acs.est.2c08855

Zhang, X. M., Johnston, E. R., Barberán, A., Ren, Y., Wang, Z. P., & Han, X. G. (2018). Effect of intermediate disturbance on soil microbial functional diversity depends on the amount of effective resources. *Environmental Microbiology*, *20*(10), 3862–3875. https://doi.org/10.1111/1462-2920.14407

Zheng, B. X., Zhu, Y. G., Sardans, J., Penuelas, J., & Su, J. Q. (2018). QMEC: A tool for high-throughput quantitative assessment of microbial functional potential in C, N, P, and S biogeochemical cycling. *Science China Life Sciences*, *61*(12), 1451–1462. https://doi.org/10.1007/s11427-018-9364-7

Zhou, J., Wu, Y. H., Turner, B. L., Sun, H. Y., Wang, J. P., Bing, H. J., et al. (2019). Transformation of soil organic phosphorus along the Hailuogou post-glacial chronosequence, southeastern edge of the Tibetan Plateau. *Geoderma*, *352*, 414–421. https://doi.org/10.1016/j.geoderma.2019.05.038

Zhou, J. C., Zhang, L., Feng, G., & George, T. S. (2022). Arbuscular mycorrhizal fungi have a greater role than root hairs of maize for priming the rhizosphere microbial community and enhancing rhizosphere organic P mineralization. *Soil Biology and Biochemistry*, *171*, 108713. https://doi.org/10.1016/j.soilbio.2022.108713